Experimental Study on Coupling Characteristics of Cutting Heat and Cutting Vibration Under Different Tool Wear States

Songyuan Li
Jiangsu Normal University
Shuncai Li (zsclsc@263.net)
Jiangsu Normal University
Yuting Hu
Jiangsu Normal University
Eugene Popov
Petersburg Polytechnic University

Research Article

Keywords: Different tool wear states, Cutting temperature change, Cutting vibration, Cutting parameters, Coupling characteristics

Posted Date: March 1st, 2021

DOI: https://doi.org/10.21203/rs.3.rs-249143/v1

Experimental study on coupling characteristics of cutting heat and cutting vibration under different tool wear states

Songyuan Li [a], Shuncai Li [b], Yuting Hu[b], Eugene Popov [c]

a. School of Mechanical and Electrical Engineering, Jiangsu Normal University, Xuzhou Jiangsu 221116, China

b. JSNU-SPBPU Institute of Engineering, Jiangsu Normal University, Xuzhou Jiangsu 221116, China

c. Higher school of applied physics and space technologies, Petersburg Polytechnic University, Saint-Petersburg 1952151, Russia

(**Correspondence author:** Shuncai Li **E-mail address:** zsclsc@263.net.)

Abstract: The thermo-mechanical-vibration coupling characteristics of turning system has always been an important research topic in the field of machining, and the material, states and performance of cutting tools will directly affect this coupling characteristics. In this paper, a synchronous testing system for cutting temperature and cutting vibration is built to collect the cutting temperature and cutting vibration near the tip of three worn tools D1 (new blade), D2 (moderately worn blade) and D3 (severely worn blade). Based on the test data and the grey correlation theory, the coupling characteristics of cutting temperature rise and cutting vibration of tools in different wear states are analyzed. Based on the experimental data and least square method, (1) the regression model of cutting temperature rise about cutting vibration and cutting parameters (2) the regression model of cutting vibration about cutting temperature rise and cutting parameters have been established respectively. The undetermined parameters and correlation coefficients are obtained by MATLAB software programming. The research show that the coupling of cutting heat and cutting vibration of tools D1 and D2 is one-way coupling, that is, cutting vibration significantly affects cutting heat, but cutting heat has little effect on cutting vibration, while the coupling of cutting heat and cutting vibration of tool D3 is a bidirectional coupling.

Keywords: Different tool wear states; Cutting temperature change; Cutting vibration; Cutting parameters; Coupling characteristics

Nomenclature

n	The spindle speed	$\overline{a}_{\text{RMS-a}}$ (axial)	The measured root-mean-square value of three-way vibration acceleration in turning
v	The cutting speed	$\overline{a}_{\text{RMS-r}}$ (radial)	
v_{f}	The feed speed	$\overline{a}_{\text{RMS-t}}$ (tangential)	
a_{p}	The cutting depth	$\tilde{a}_{\text{RMS-a}}$ (axial)	The predicted root-mean-square value of three-way vibration acceleration in turning
$\Delta\overline{T}$	The measured mean temperature rise	$\tilde{a}_{\text{RMS-r}}$ (radial)	

$\Delta\tilde{T}_a$ (axial)		$\tilde{a}_{\text{RMS-t}}$ (tangential)	
$\Delta\tilde{T}_r$ (radial)	The predicted mean three-way temperature rise	D1	The new blade
$\Delta\tilde{T}_t$ (tangential)		D2	The moderately worn blade
a_{a} (axial)		D3	The severely worn blade
a_r (radial)	The three-way acceleration	R_{D1} R_{D2} R_{D}	The grey relational analysis for tool D1, D2, D3
a_{t} (tangential)		C x, y, z, w	The undetermined coefficients
P	The probability value of zero correlation	R	The correlation coefficient
I	The radiant energy per unit distance squared of the object radiation unit	ε	The emissivity,
		T	The temperature of object in Kelvin,
σ	Stefan's constant	T_{a}	The temperature of ambient surrounding in Kelvin

1 Introduction

In the turning process, there is relative friction between the tool and the workpiece, which not only causes the continuous rise of temperature in the tool and in the work-piece, but also produces serious cutting vibration, which speeds up the tool wear. The tool wear will accelerate the rising speed of cutting temperature, shorten the tool life, and reduce the strength of the work-piece and the surface quality. In flexible production system, if the tool wear states is not known or the worn tool cannot be replaced in time, the production efficiency will be reduced [1].

There are a lot of literatures on the influence of cutting tool material, geometric parameters, processing conditions and cutting parameters on cutting temperature. Zhang et al. [2] studied the influence of geometric parameters of cutting tools on cutting temperature, and found that the cutting temperature will also rise when the rake angle and edge angle increase. Majumdar et al. [3] studied the influence of turning conditions, tool geometry and temperature distribution of tool material on tool life, established a finite element model, and obtained the range of turning conditions for machining high-speed steel. Karaguzel, Cui and Chinchanikar [4-6] studied the correlation between cutting parameters and cutting temperature. Liu and Li [7-8] studied the tool temperature in the turning process of titanium alloy, and found the interaction between the degree of tool wear and the cutting temperature.

Zhang et al. [9] studied the change of cutting temperature with different cutting parameters for titanium matrix composite tool, and found that the lower the cutting speed, the higher the cutting temperature. analyzed the wear mechanism of titanium alloy cutting tools, and determined the interaction between cutting temperature and tool wear. Shi [10] and Qu [11] established a mathematical model of cutting temperature and cutting force to prove the correlation between cutting temperature and cutting parameters. Shah et al. [12] studied the influence of cutting parameters on the cutting temperature of Ti-6Al-4V cutting process through particle swarm optimization algorithm. Turkes et al. [13] used the finite element analysis to calculate the cutting parameters, and found that the temperature distribution of cutting tools and processing materials through the parameters. Luo and Maroju [14-15] studied the cutting temperature by vibration assisted turning.

Taking cutting vibration as the research object, some scholars study the influence of cutting parameters, cutting force, machine structure and processing conditions on the vibration through experiments and regression models. Li, Chanda, Deshpande and Chen [16-19] analyzed the influence of cutting and cutting parameters on cutting vibration through experiments. Hu et al. [20] studied the influence of lathe internal structure on cutting vibration, established the dynamic model of turning system based on ER damper, and found that the cutting vibration reduction effect was different under different cutting parameters. Cui et al. [21] proved that the cutting parameters has a direct impact on the cutting force and cutting vibration, and the cutting vibration can be controlled by changing the cutting parameters. Chuan et al. [22] tried to monitor the wear of cutting tool by cutting vibration. Ozbekp et al. [23] used three different cutting speeds to evaluate the tool vibration amplitude under dry cutting conditions. The results showed that the faster the cutting speed, the more the vibration amplitude of the tool decreased. Prasad et al. [24] studied the relationship between tool vibration and tool wear, and found that the change of the two will accelerate the speed of tool wear. Thomas et al. [25] collected and analyzed the cutting vibration data of low carbon steel under different cutting parameters and tool geometric parameters. Ghosh et al. [26] used coated cemented carbide tool CTC 1135 for finish machining to study the influence of cutting parameters on cutting vibration, and found that the influence of cutting speed on vibration is small. Upadhyay et al. [27] established a multiple regression model for acceleration amplitude through three-way vibration, and analyzed cutting parameters and vibration acceleration amplitude.

Some scholars have also studied the influence of different machining conditions on tool wear through experiments. Liu et al. [28] found that the tool wear of ultrasonic assisted

milling is less than that of conventional milling. Mou et al. [29] compared the effects of liquid nitrogen machining and dry machining on tool wear, and found that liquid nitrogen machining reduced tool side wear. Das et al. [30] studied tool wear through variance analysis, and obtained that tool wear increased with the increase of cutting parameters. Fang et al. [31] found that increasing coolant pressure can reduce tool wear. UPase and Dou [32-33] collected vibration signals through artificial neural network model to predict tool wear.

It is known from the above literature that most scholars have studied the influence of cutting parameters on cutting vibration and cutting temperature, and have also analyzed the influence of tool wear states on cutting temperature and cutting vibration. However, the research findings of coupling relationship among cutting parameters, cutting temperature and cutting vibration under different tool wear states are not rich. In this paper, the cutting temperature and three-way cutting vibration near the tool tip under the corresponding cutting parameters are obtained through the cutting test under different tool wear states. Based on the test data, the relative correlation analysis between the cutting parameters, cutting temperature and cutting vibration of the three kinds of cutting tools is calculated by grey system theory. Then the cross-correlation model of cutting temperature and cutting vibration is established based on experiments to analyze the coupling characteristics between cutting temperature rise, cutting vibration and cutting parameters under different tool wear states. The specific research process is shown as Fig. 1.

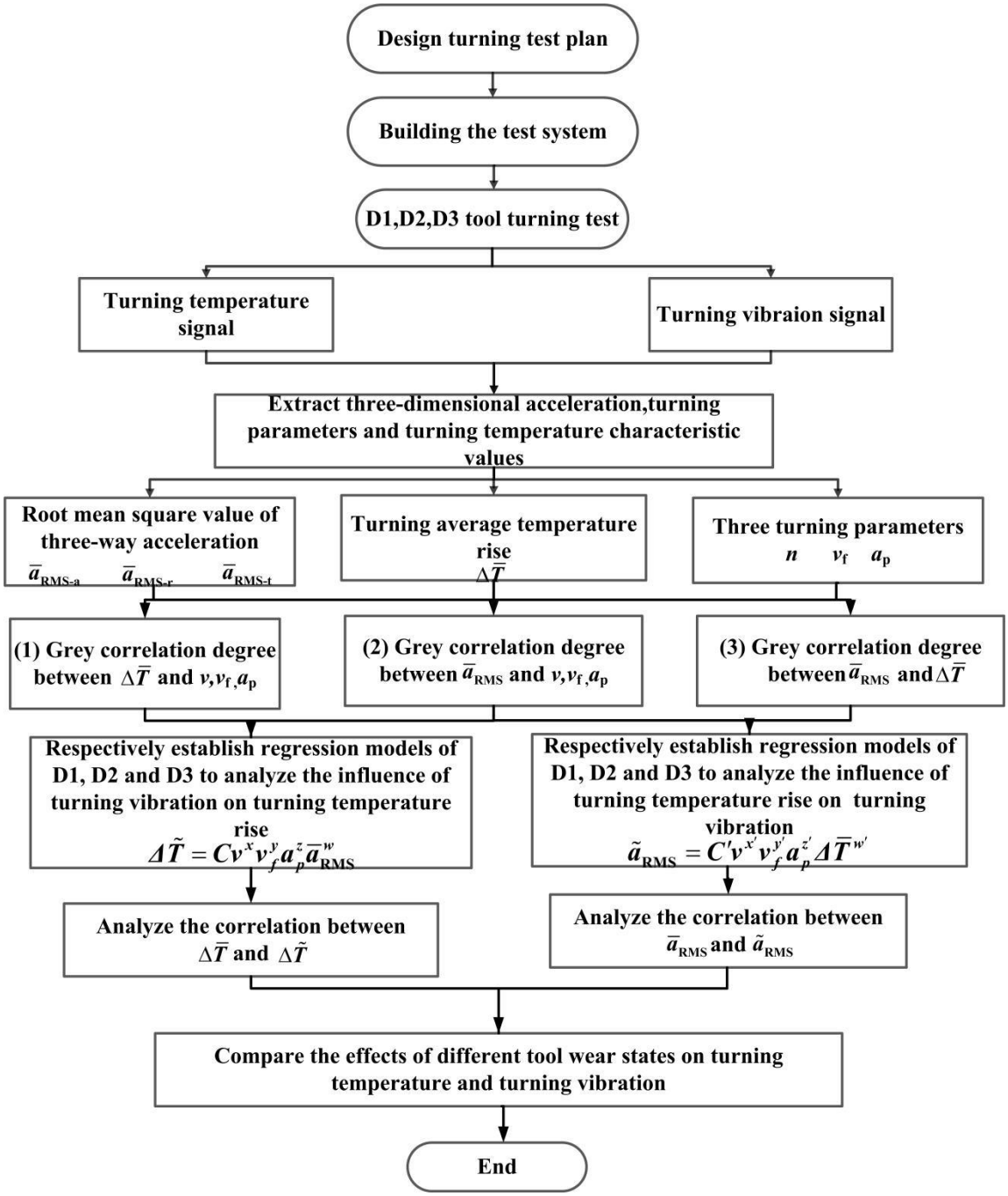

Fig.1 Research technology roadmap

2 Experimental designs

2.1 Experiments equipment

As shown in Fig.2, CJK6136-MATE-360×570 CNC lathe is used in this test, and the test workpiece is 45mm aluminum alloy bar. OS523E-2 hand-held infrared thermometer is used for the temperature acquisition instrument. The cutting temperature measurement system is composed of infrared thermometer, OMEGASOFT OS5xx Access acquisition software and

computer, which can measure and display the cutting temperature in real time. The YD-21 piezoelectric three-directional acceleration sensor, WS-2402 vibration signal acquisition instrument, DAQ signal acquisition and processing software and computer are used to form a vibration measurement and analysis system. The cemented carbide coated inserts with three wear states, D1 (new blade), D2 (moderately worn blade) and D3 (severely worn blade) were used in the test. The test system is shown in Fig.2.

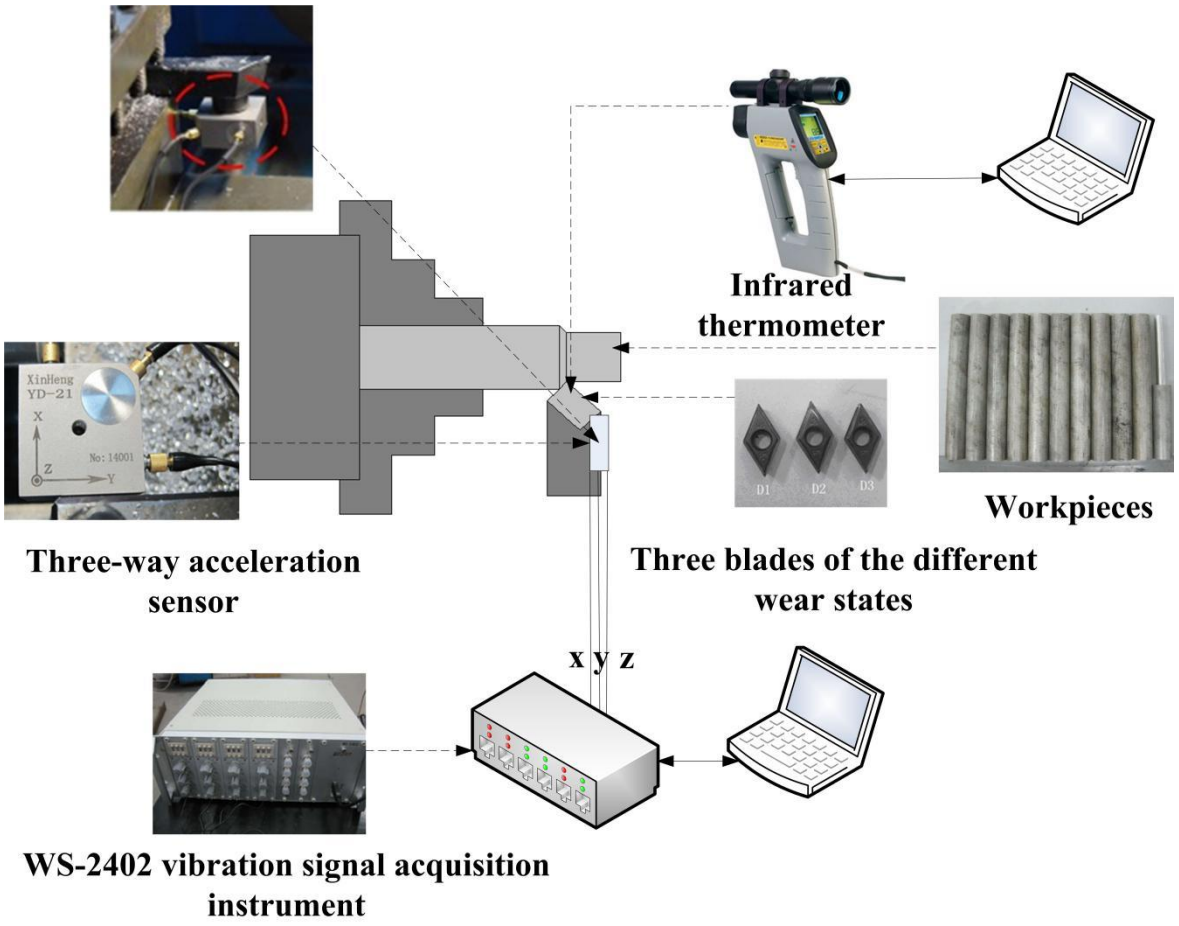

Fig. 2 Cutting test system

2.2 Experiments plan

In this experimental design, D1, D2 and D3 tools are used to carry out the dry turning tests on aluminum rods with a diameter of 45mm.

In the cutting experiment, the spindle speed n is designed as four levels: 800 r / min, 1200r / min, 1600r / min and 2000r / min, and the feed speed v_f is designed as three levels: 40mm / min, 80mm / min, 160mm / min, and the cutting depth has three levels :0.3mm, 0.5mm and 0.8mm. In order to prevent tests failure, the cutting experiments corresponding to each group of cutting parameters were conducted twice, and the time of each cutting test is designed as 1 minute. The specific parameters are shown in Table 1.

Table 1 Cutting test scheme

v_f=40 mm/min			v_f=80 mm/min			v_f=160 mm/min		
test number.	n (r/min)	a_p (mm)	test number.	n (r/min)	a_p (mm)	test number.	n (r/min)	a_p (mm)
1	800	0.3	13	800	0.3	25	800	0.3
2	1200	0.3	14	1200	0.3	26	1200	0.3
3	1600	0.3	15	1600	0.3	27	1600	0.3
4	2000	0.3	16	2000	0.3	28	2000	0.3
5	800	0.5	17	800	0.5	29	800	0.5
6	1200	0.5	18	1200	0.5	30	1200	0.5
7	1600	0.5	19	1600	0.5	31	1600	0.5
8	2000	0.5	20	2000	0.5	32	2000	0.5
9	800	0.8	21	800	0.8	33	800	0.8
10	1200	0.8	22	1200	0.8	34	1200	0.8
11	1600	0.8	23	1600	0.8	35	1600	0.8
12	2000	0.8	24	2000	0.8	36	2000	0.8

2.3 Test procedure

During the cutting test, the cutting temperature and three-way acceleration are collected at the same time, the test procedures are as follows:

(1) Prepare the work-piece: select the aluminum bar with the diameter of 45mm after rough machining as the test work-piece;

(2) Connect and check temperature measurement equipment: connect the infrared thermometer to the personal computer with a special data line, and turn on the switch of the infrared thermometer, and then keep the infrared thermometer in acquisition locked state. Emissivity of infrared thermometer is 0.95. The temperature near the tool tip is collected and recorded by the infrared thermometer and the temperature measurement software in the computer;

(3) Connect and check three-way vibration measuring equipment: Fix the three-way acceleration sensor on the lower surface of the tool handle near the tool tip through the magnetic base. The three outputs of the three-way sensor are respectively connected to the 9, 10 and 11 channels of WS-2402 vibration measurer, and the WS-2402 vibration measurer is connected with the computer by a special data line. Then turn on the power of the WS-2402 vibration measurer and open the corresponding vibration signal acquisition software in the computer to collect and record the signals of the three-way vibration acceleration;

(4) Carry out the cutting experiments: According to the cutting parameters set in Table 1,

the cutting tests were completed one by one and at the same time the signals of the cutting temperature and three-way vibration acceleration are collected and recorded synchronously. After all the tests were finished, switch off the power.

3 Test results and analysis

3.1 Time curve of cutting vibration and cutting temperature of three tools

By the time domain analysis, the average value of cutting temperature rise in each cutting test can be obtained. As a representative, Fig.3 gives the curves of cutting temperature with time for tools D1, D2 and D3 at n = 1200r / min, v_f = 80 mm / min, a_p = 0.3mm.

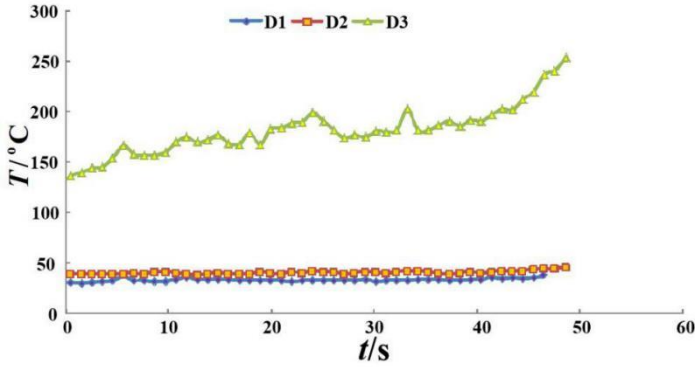

Fig. 3 Time curves of cutting temperature of three tools（at n=1200r/min, v_f=80 mm/min, a_p=0.3mm）

By vibration signal acquisition and analysis system, the time-domain curves of three-way vibration acceleration signals can be obtained. And for the three-way vibration acceleration, its maximum value, root-mean-square and so on can be obtained through time-domain analysis. Table 2 represents the time-history curves of three-way vibration acceleration for tools D1, D2 and D3 at n = 800r / min, v_f = 80 mm / min, a_p = 0.3mm.

Table 2 Time curves of cutting vibration for three tools（at n=800r/min, v_f=80 mm/min, a_p=0.3mm）

Cutter tool	a_a (m/s^2) (axial)	a_r (m/s^2) (radial)	a_t (m/s^2) (tangential)
D1	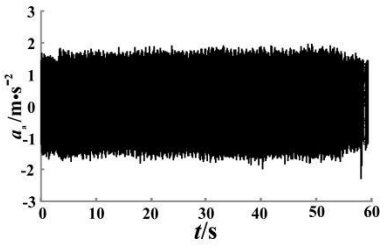	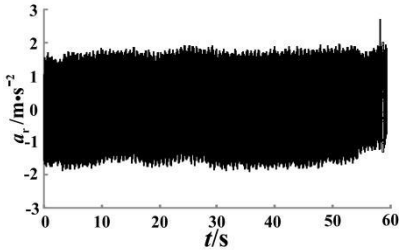	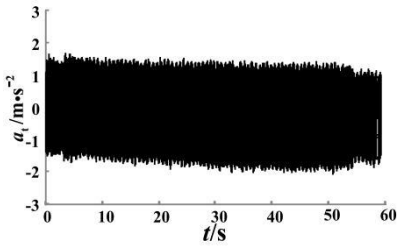
D2	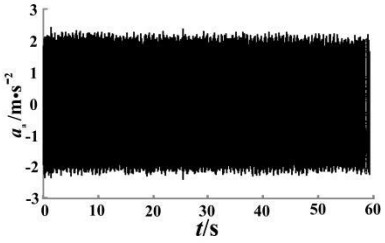	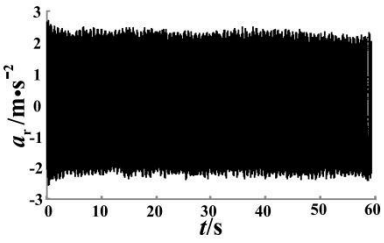	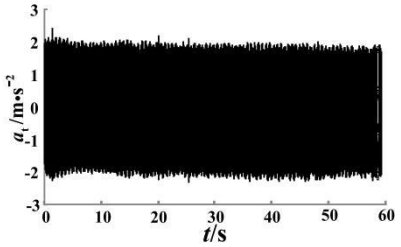
D3	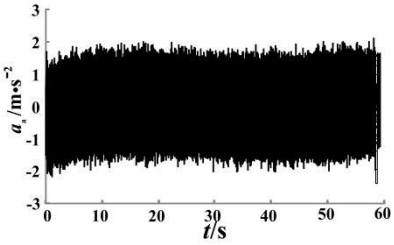	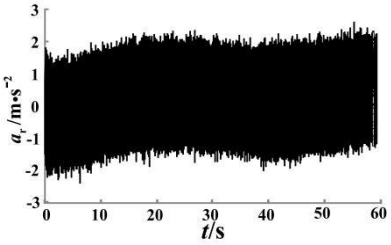	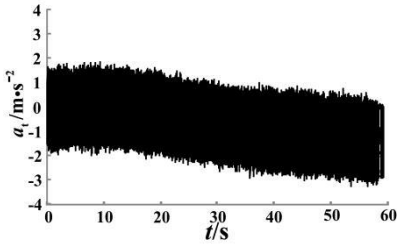

During the test, we found that the cutting temperature of severely worn tool increases sharply, and the spark sputtering phenomenon occurs for many times, and the sensor transmission line is burned out, which leads to the test interruption. Therefore, this paper mainly gives the experimental data of tools D1 and D2, and only a part of the test data of severely worn tool D3 are shown in Table 3.

In each test, the diameter of the work-piece is different and the cutting speed is also different. The cutting speed v can be obtained by the following formula.

$$v = \frac{\pi n d}{60}$$

Since the cutting test is continuous, the temperature of the tool is higher than the indoor environment temperature after each cutting test, so the initial temperature of the tool in each cutting test is different. Therefore, in the later temperature signal analysis $\Delta\overline{T}$， namely the average value of the difference between the actual measured temperature at each time and the initial temperature of each test is extracted as the characteristic value of, , and $\overline{a}_{\text{RMS-a}}$， $\overline{a}_{\text{RMS-r}}$ and $\overline{a}_{\text{RMS-t}}$ (the root-mean-square values of the three-way vibration acceleration) are selected

as the characteristic values of vibration analysis. Combining cutting parameters, establish a fitting formula about the predicted mean value $\Delta\tilde{T}$ of temperature rise and a fitting formula about the predicted three-way acceleration root-mean-square $\tilde{a}_{\mathrm{RMS}}$. Calculate the correlation between the predicted mean value $\Delta\tilde{T}$ of temperature rise and the actual measured value $\Delta\overline{T}$ of temperature rise and the correlation between the fitting value of the three-dimensional acceleration root-mean-square $\tilde{a}_{\mathrm{RMS}}$ and the actual measured value of the three-directional acceleration root-mean-square $\overline{a}_{\mathrm{RMS}}$ by MATLAB, and the coupling characteristics of cutting temperature and cutting vibration under the condition of tool wear are analyzed.

3.2 Influence of cutting parameters on cutting temperature rise under different tool wear states

According to Table 3, first by single variable analysis method we can compare and analyze the change rules of $\Delta\overline{T}$ for three kinds of tools D1, D2 and D3 under different levels of cutting parameters. Fig. 4 shows the $\Delta\overline{T}$ comparison between tools D1, D2 and D3 with the changing of spindle speed, feed rate and cutting depth.

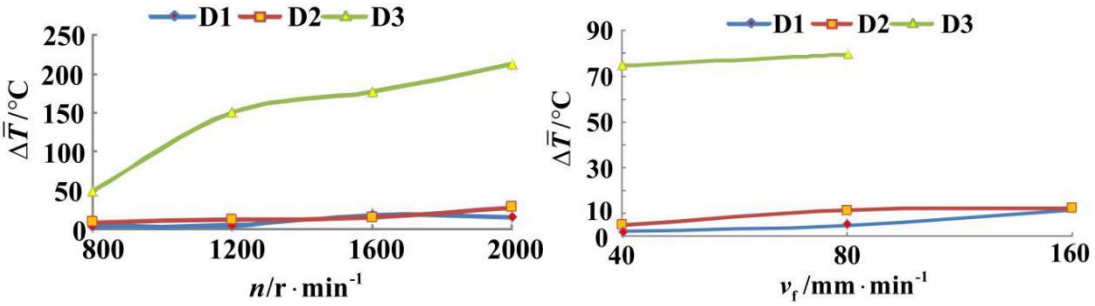

(a) different n(at v_f =80 mm/min , a_p =0.3 mm) (b) different v_f (at n=800 r/min , a_p =0.3 mm)

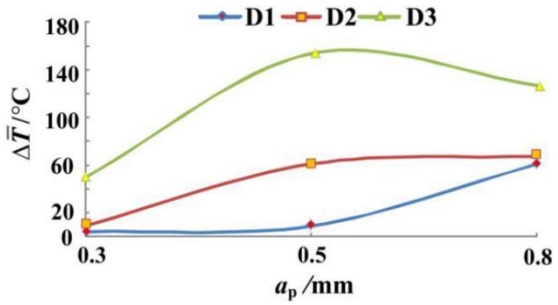

(c) different a_p(at n=800 r/min ,v_f=80 mm/min)

Fig. 4 Comparison curve of cutting temperature rise of 3 kinds of tools under different cutting parameters

Table 3 Cutting test data of different tools

test number	n(r/min)	v(mm/s)	a_p (mm)	v_f(mm/min)	$\Delta\bar{T}$ (□)			$\bar{a}_{RMS\text{-}a}$ (m/s^2)			$\bar{a}_{RMS\text{-}r}$ (m/s^2)			$\bar{a}_{RMS\text{-}t}$ (m/s^2)		
					D1	D2	D3	D1	D2	D3	D1	D2	D3	D1	D2	D3
1	800	1884	0.3	40	2.01	4.15	79.59	0.80	1.05	0.97	0.88	0.79	1.01	0.81	1.03	0.96
2	1200	2750.64	0.3	40	3.29	9.84	70.50	0.79	0.76	1.83	1	0.78	1.9	0.83	0.89	1.81
3	1600	3567.04	0.3	40	5.02	6.26	138.2	0.7	0.83	1.09	0.78	0.88	1.14	0.73	0.84	1.57
4	2000	4333.2	0.3	40	7.49	4.56	119.77	0.84	0.77	1.5	0.93	0.81	1.56	0.86	0.79	1.52
5	800	1683.04	0.5	40	9.36	6.98	152.69	0.73	0.78	1.99	0.85	0.85	2.05	0.81	0.79	2.06
6	1200	2398.96	0.5	40	11.88	6.48	204.49	1.09	0.87	1.69	1.24	0.92	1.73	1.17	0.92	1.83
7	1600	3031.15	0.5	40	13.14	2.17	199.52	1.11	0.83	1.16	1.22	0.80	1.16	1.28	1.01	1.31
8	2000	3579.6	0.5	40	12.46	8.07	189.41	0.55	0.82	1.39	0.62	0.83	1.35	0.61	0.78	1.48
9	800	1348.11	0.8	40	14.02	2.57	125.08	0.83	1.18	1.24	0.95	1.13	1.29	0.96	1.21	1.47
10	1200	1821.2	0.8	40	21.22	7.30	103.84	0.73	1.21	1.15	0.86	1.09	1.22	0.78	1.39	1.13
11	1600	2160.32	0.8	40	19.76	8.57	74.8	0.80	0.82	0.88	0.95	0.87	0.96	0.92	0.80	0.91
12	2000	2365.47	0.8	40	28.12	10.85	67.00	0.97	0.82	0.69	1.07	0.82	0.71	1.27	0.79	0.88
13	800	1884	0.3	80	4.17	8.62	48.57	0.76	1.00	0.70	0.83	1.09	0.80	0.80	1.03	1.08
14	1200	2750.64	0.3	80	5.50	13.14	148.88	1.27	1.44	0.79	1.39	1.57	1.07	1.33	1.51	1.36
15	1600	3567.04	0.3	80	19.04	15.38	176.98	0.87	0.97	0.99	1.03	1.06	1.11	0.99	1.01	1.45
16	2000	4333.2	0.3	80	15.06	27.98	210.44	0.86	0.72	1.09	1.01	0.78	1.62	1.27	0.74	1.64
17	800	1683.04	0.5	80	8.85	58.97	292.6	0.77	0.80	1.11	0.84	0.91	1.53	0.84	0.83	1.41
18	1200	2398.96	0.5	80	27.25	55.09		0.7	0.63		0.72	0.68		0.78	0.75	
19	1600	3031.15	0.5	80	62.88	59.88		0.97	0.91		1.06	0.99		1.15	0.99	
20	2000	3579.6	0.5	80	110.34	77.82		0.77	0.71		0.92	0.77		0.81	0.75	
21	800	1348.11	0.8	80	61.42	67.53		1.01	0.61		1.18	0.67		1.13	0.65	

22	1200	1821.2	0.8	80	60.71	68.00	0.79	0.93	0.98	1.01	1	1.05
23	1600	2160.32	0.8	80	78.52	73.16	0.69	0.86	0.84	0.97	1.24	1.04
24	2000	2198	0.8	80	135.02	209.77	0.65	1.03	0.90	1.12	0.93	1.1
25	800	1884	0.3	160	9.51	9.88	0.80	0.49	0.90	0.53	0.93	0.51
26	1200	2750.64	0.3	160	13	13.86	0.67	0.53	0.73	0.58	0.89	0.68
27	1600	3567.04	0.3	160	19.7	19.08	0.84	0.58	0.90	0.64	0.93	0.61
28	2000	4333.2	0.3	160	40.93	65.34	0.87	0.49	0.96	0.54	0.96	0.52
29	800	1683.04	0.5	160	60.63	91.40	0.50	0.55	0.55	0.71	0.55	0.63
30	1200	2398.96	0.5	160	84.81	85.08	0.66	0.54	1.29	0.62	0.97	0.90
31	1600	3031.15	0.5	160	77.29	82.67	0.71	0.56	0.81	0.61	0.96	0.63
32	2000	3579.6	0.5	160	68.51	81.69	0.72	0.52	0.79	0.58	0.91	0.56
33	800	1348.12	0.8	160	86.15	123.33	0.90	0.58	1	0.82	1.02	0.62
34	1200	1821.2	0.8	160	87.42	111.82	0.87	0.61	1.77	0.74	1.05	0.65
35	1600	2160.32	0.8	160	93.7	109.54	0.80	0.60	1.98	0.68	0.89	0.67
36	2000	2365.47	0.8	160	98.21	104.12	0.68	0.54	1.14	0.59	0.96	0.57

According to Fig.4 (a), with the increase of spindle speed, $\Delta\overline{T}$ of tool D3 rises sharply, which is far greater than that of tools D1 and D2. While for tools D1 and D2, their temperature rise difference is not significant.

According to Fig.4 (b), with the increase of feed rate, the $\Delta\overline{T}$ curve of tools D1 and D2 shows a slow upward trend, and the $\Delta\overline{T}$ of tool D3 is much higher than that of tools D1 and D2. It is worth mentioning that when the feed speed of tool D3 reaches 160mm/min, the cutting temperature is too high and the sensor transmission line is burned off, resulting in the missing data of tool D3.

According to Fig.4 (c), the $\Delta\overline{T}$ of the three tools increases sharply with the increase of cutting depth, and the more serious the tool wear is, the faster $\Delta\overline{T}$ rises and the maximum $\Delta\overline{T}$ reaches 153 □.

In conclusion, the temperature rise $\Delta\overline{T}$ of tool D3 increases more than that of tools D1 and D2, and when the cutting depth is large, the temperature rise $\Delta\overline{T}$ of tool D3 with severe wear is more obvious.

3.3 Influence of tool wear states on cutting vibration

Compare the root-mean-square values of three direction accelerations, $\overline{a}_{\text{RMS-a}}$, $\overline{a}_{\text{RMS-r}}$, $\overline{a}_{\text{RMS-t}}$ for three tools D1, D2, D3 under the same cutting parameters as shown in Fig. 5 (a)-(c), according to Fig. 6, the $\overline{a}_{\text{RMS-a}}$, $\overline{a}_{\text{RMS-r}}$, $\overline{a}_{\text{RMS-t}}$ curves of three tools are basically similar. In most tests, the root-mean-square value of acceleration for tools D3 and D1 is greater than that of tool D2. The wear of tool D1 is small and the contact area between tool transition surface and work-piece is small, which accelerates tool wear and leads to relatively severe vibration. While for tool D3 its cutting vibration is serious due to serious wear.

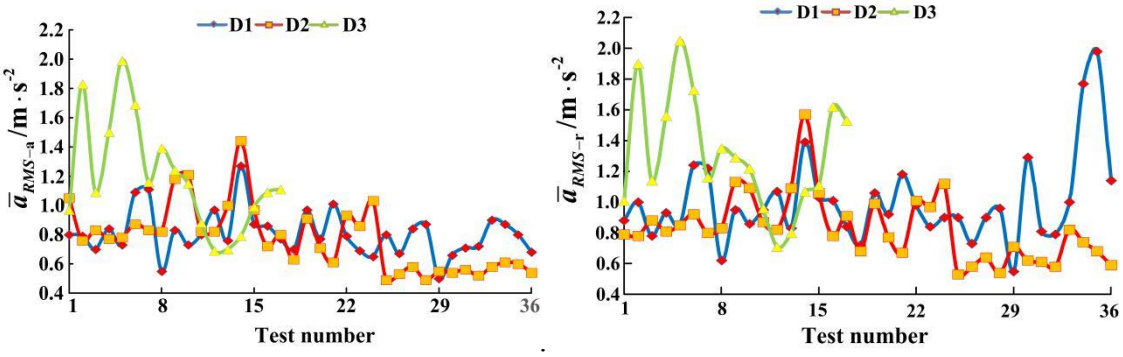

(a) axial acceleration (b) radial acceleration

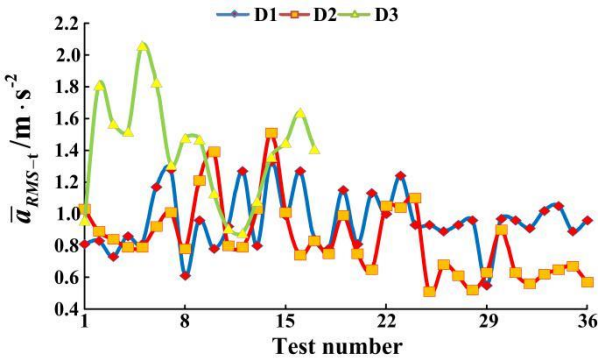

(c) tangential acceleration

Fig. 5 Comparing curves of acceleration mean square of all tests for three tools

3.4 Grey correlation analysis of cutting temperature rise, cutting vibration and cutting parameters

According to the relationship between the series change rate relative to the starting point, the grey relational analysis can judge whether the relationship between series is close. The closer the change rate is, the greater the relative correlation is. Combined with the test data, the grey relational analysis can be used to find the factors which have the greatest influence on the cutting temperature rise and the cutting vibration, and analyze the correlation between the cutting temperature rise and the cutting vibration. The grey relational analysis value [34] needs to be calculated by the relative grey relational analysis theory, and the grey relational analysis related to the three tools is represented by R_{D1}, R_{D2} and R_{D3} respectively. Firstly, the grey correlation between cutting temperature rise, cutting vibration and cutting parameters is analyzed, and then the grey correlation between cutting temperature rise and cutting vibration is analyzed.

3.4.1 Grey relational analysis of cutting temperature rise and cutting parameters

According to the cutting parameters v, v_f, a_p and the average value of temperature rise $\Delta\overline{T}$ of three kinds of cutting tools in each test, the grey relational analysis between the cutting temperature rise of three kinds of cutting tools and cutting parameters is calculated, and which cutting parameters have the most significant influence on the tool temperature rise is analyzed. The calculation results are shown in Table 4.

Table 4 Grey relational analysis between cutting temperature and cutting parameters

The mean temperature rise	Cutting parameters	Relative grey relational analysis		
		R_{D1}	R_{D2}	R_{D3}
$\Delta\overline{T}$	v	0.77	0.78	0.94
	v_f	0.87	0.88	0.89

	a_p	0.83	0.84	0.97

According to Table 4,we have: (1) The correlation coefficients between the average temperature rise and the cutting parameters of the three kinds of cutting tools are all greater than 0.75, which indicates that cutting parameters have great influence on the change of cutting temperature; (2) compare the correlation between average cutting temperature rise $\Delta\bar{T}$ and cutting parameters for three tools under the same cutting parameters, we can obtain R_{D3}> R_{D2}> R_{D1} The average cutting temperature rise $\Delta\bar{T}$ of severely worn tools has the highest correlation with cutting parameters., so the change of cutting parameters will significantly affect the cutting temperature rise of severely worn tools, but it has little effect on the new tools; (3) Among the three cutting parameters, for tools D1 and D2, the average temperature rise $\Delta\bar{T}$ has the highest correlation with the feed rate v_f, and the lowest correlation with the cutting speed v. Therefore, the feed rate has the greatest impact on the cutting temperature of tools D1 and D2, and the cutting speed has the smallest impact. For tool D3, the average temperature rise $\Delta\bar{T}$ has the highest correlation with the cutting depth a_p, and the lowest correlation with the cutting speed v. Therefore, the cutting depth has the greatest effect on the cutting temperature of tool D3, while the feed rate has the least effect.

3.4.2 Grey relational analysis of cutting vibration and cutting parameters

According to the cutting parameters and $\bar{a}_{RMS\text{-}a}$, $\bar{a}_{RMS\text{-}r}$, $\bar{a}_{RMS\text{-}t}$ (the three-way acceleration root-mean-square values of the three kinds of cutting tools in each test), the grey relational analysis between $\bar{a}_{RMS\text{-}a}$, $\bar{a}_{RMS\text{-}r}$, $\bar{a}_{RMS\text{-}t}$ and the cutting parameters for the three kinds of cutting tools is calculated as shown in Table 5. According to Table 5, we can see that cutting parameters have the most significant influence on the acceleration root-mean-square value.

Table 5 Grey relational analysis between cutting vibration and cutting parameters

Root-mean-square value of three-way acceleration	Cutting parameters	Relative grey relational analysis		
		R_{D1}	R_{D2}	R_{D3}
$\bar{a}_{RMS\text{-}a}$	v	0.83	0.73	0.93
	v_f	0.74	0.68	0.98
	a_p	0.78	0.70	0.89
$\bar{a}_{RMS\text{-}r}$	v	0.90	0.86	0.95
	v_f	0.79	0.76	0.99
	a_p	0.89	0.80	0.92
$\bar{a}_{RMS\text{-}t}$	v	0.92	0.75	0.99

	v_f	0.81	0.70	0.93
	a_p	0.85	0.71	0.97

According to Table 5, (1) we can compare the correlation between root-mean-square value of acceleration $\overline{a}_{RMS}$ and cutting parameters for three tools under the same cutting parameters, we can obtain R_{D3}> R_{D1}> R_{D2}. The $\overline{a}_{RMS}$ of severely worn tool has the highest correlation with cutting parameters, but the correlation degree of the moderately worn tools is the lowest. (2) For the same tool, we can compare which direction of vibration acceleration has the highest correlation with the same cutting parameters. It can be seen that almost the axial vibration acceleration of the three tools has the lowest correlation with the same turning parameter, and the tangential correlation is the highest; (3) For the vibration in a certain direction of the same tool, we can also compare this directional vibration has the highest correlation with which turning parameter. It can be seen that for tools D1 and D2, three-way vibration has the highest correlation with the turning speed v, and the lowest correlation with the feed speed v_f. For tool D3, the axial and radial vibrations have the highest correlation with the feed speed v_f, and the lowest correlation with the cutting depth a_p. The tangential vibration has the highest correlation with the cutting speed v. The lowest correlation is given to the speed v_f.

3.4.3 Grey relational analysis between cutting temperature rise and cutting vibration

Based on the grey relational analysis, the correlation between the average cutting temperature rise $\Delta\overline{T}$ and $\overline{a}_{RMS\text{-}a}$, $\overline{a}_{RMS\text{-}r}$, $\overline{a}_{RMS\text{-}t}$ of the three tools under given cutting parameters is analyzed. The corresponding calculation results are shown in Table 6.

Table 6 Grey relational analysis between cutting temperature and cutting vibration

The mean temperature rise	Root-mean-square value of three-way acceleration	Relative grey relational analysis		
		R_{D1}	R_{D2}	R_{D3}
$\Delta\overline{T}$	$\overline{a}_{RMS\text{-}a}$	0.68	0.65	0.87
	$\overline{a}_{RMS\text{-}r}$	0.71	0.70	0.90
	$\overline{a}_{RMS\text{-}t}$	0.72	0.66	0.95

According to Table 6, (1) compare the correlation between average cutting temperature rise $\Delta\overline{T}$ and root-mean-square value of acceleration $\overline{a}_{RMS}$ for three tools under the same cutting parameters, we can obtain R_{D3}> R_{D1}> R_{D2}. The average cutting temperature rise $\Delta\overline{T}$ of severely worn tools has the highest correlation with the root-mean-square value of acceleration $\overline{a}_{RMS}$, so the change of cutting vibration will significantly affect the cutting

temperature of severely worn tools, but the effect on moderately worn tools is small. (2) For the same tool, which direction vibration acceleration has the highest correlation with cutting temperature rise can be compared. It can be seen that for tools D2 and D3, the correlation between cutting temperature rise $\Delta\overline{T}$ and radial vibration $\overline{a}_{\text{RMS-}t}$ is the highest, and that with axial vibration $\overline{a}_{\text{RMS-}a}$ is the lowest. For tool D1, the correlation between cutting temperature rise $\Delta\overline{T}$ and tangential vibration $\overline{a}_{\text{RMS-}r}$ is the highest, and that with axial vibration $\overline{a}_{\text{RMS-}a}$ is the lowest.

The above analysis shows that there is a certain correlation between the change of cutting temperature and cutting vibration. According to the following Stephen-Boltzmann's law formula (1) and the area of measured temperature domain and emissivity and temperature of ambient surrounding,

$$I=\varepsilon\sigma(T^4-T_{\text{a}}^4) \tag{1}$$

Where, I- the radiation energy per unit area of the object radiation unit(W/m^2), ε -emissivity; σ - Stefan's constant and $\sigma=5.6696\times10^{-8}\,\text{W}\cdot\text{m}^{-2}\cdot\text{K}^{-4}$; T-temperature of object in Kelvin (K), T_{a} -temperature of ambient surrounding in Kelvin(K).

By the measured cutting temperature T, T_{a} and temperature measurement area, according to Eq.(1), we can calculate the cutting heat I radiated per unit time near the contact between the cutting tool and the workpiece. Therefore, the correlation between cutting heat and cutting vibration can be obtained by analyzing the correlation between cutting temperature rise and cutting vibration. The following specifically studies the coupling characteristics of cutting temperature rise and cutting vibration.

3.5 The coupling characteristics of cutting temperature rise and cutting vibration of tools with different wear states

In order to comprehensively analyze the coupling characteristics of cutting temperature rise, cutting vibration and cutting parameters, the nonlinear regression analysis based on the least square method is adopted because the grey correlation analysis method is only suitable for studying the correlation degree of two groups of data. The regression models of (1) cutting vibration on cutting temperature rise and cutting parameters and (2) the regression models of cutting temperature rise on cutting vibration and cutting parameters were established respectively to analyze the mutual effects of cutting temperature rise, cutting vibration and cutting parameters.

3.5.1 The fitting model of cutting temperature rise by cutting vibration and cutting parameters

In order to analyze the effect of cutting vibration and cutting parameters on cutting temperature rise, the following uses the root-mean-square value of acceleration in a certain direction of the three-way vibration $\overline{a}_{\mathrm{RMS}}$ and three cutting parameters as independent variables to establish a fitting model for predicting the mean value of cutting temperature rise $\Delta\overline{T}$, namely

$$\Delta\tilde{T} = Cv^{x}v_{\mathrm{f}}^{y}a_{\mathrm{p}}^{z}\overline{a}_{\mathrm{RMS}}^{w} \tag{2}$$

Where $\Delta\tilde{T}$ –the fitted average value of cutting temperature rise, C, x, y, z, w – undetermined coefficients in fitting formula.

Take the logarithm operation respectively on both sides of Eq. (2), we have

$$\ln\Delta\tilde{T}=\ln C + x\ln v + y\ln v_f + z\ln a_p + w\ln\overline{a}_{\mathrm{RMS}} \tag{3}$$

The average value of the measured cutting temperature is $\Delta\overline{T}$, and the Logarithmic difference between the predicted value $\Delta\tilde{T}$ and the measured value $\Delta\overline{T}$ is as follows

$$\ln\Delta\tilde{T} - \ln\Delta\overline{T}=\ln C + x\ln v + y\ln v_f + z\ln a_p + w\ln\overline{a}_{\mathrm{RMS}} - \ln\Delta\overline{T}$$

Let $\prod$ is the sum of squares of the residual errors between the fitting value $\ln\Delta\tilde{T}$ and the measured value $\ln\Delta\overline{T}$ in each test, and the undetermined coefficients C, x, y, z, w can be obtained by solving the minimum value of $\prod$.

$$\Pi = \sum_{i=1}^{n}(\eta + x\ln v_i + y\ln v_{fi} + z\ln a_{pi} + w\ln(\overline{a}_{\mathrm{RMS}})_i - \ln\Delta\overline{T}_i)^2, \ln C = \eta \tag{4}$$

By the least square method, let $\frac{\partial\Pi}{\partial x}=0, \frac{\partial\Pi}{\partial y}=0, \frac{\partial\Pi}{\partial z}=0, \frac{\partial\Pi}{\partial w}=0, \frac{\partial\Pi}{\partial\eta}=0$, we have:

$$\frac{\partial\Pi}{\partial x}=0: x\sum_{i=1}^{n}\ln v_i^{\,2} + y\sum_{i=1}^{n}\ln v_{fi}\ln v_i + z\sum_{i=1}^{n}\ln a_{pi}\ln v_i + w\sum_{i=1}^{n}\ln(\overline{a}_{\mathrm{RMS}})_i\ln v_i + \eta\sum_{i=1}^{n}\ln v_i = \sum_{i=1}^{n}\ln v_i\ln\Delta\overline{T}_i \tag{5}$$

$$\frac{\partial\Pi}{\partial y}=0: x\sum_{i=1}^{n}\ln v_i\ln v_{fi} + y\sum_{i=1}^{n}\ln v_{fi}^{\,2} + z\sum_{i=1}^{n}\ln a_{pi}\ln v_{fi} + w\sum_{i=1}^{n}\ln(\overline{a}_{\mathrm{RMS}})_i\ln v_{fi} + \eta\sum_{i=1}^{n}\ln v_{fi} = \sum_{i=1}^{n}\ln v_{fi}\ln\Delta\overline{T}_i \tag{6}$$

$$\frac{\partial\Pi}{\partial z}=0: x\sum_{i=1}^{n}\ln v_i\ln a_{pi} + y\sum_{i=1}^{n}\ln v_{fi}\ln a_{pi} + z\sum_{i=1}^{n}\ln a_{pi}^{\,2} + w\sum_{i=1}^{n}\ln(\overline{a}_{\mathrm{RMS}})_i\ln a_{pi} + \eta\sum_{i=1}^{n}\ln a_{pi} = \sum_{i=1}^{n}\ln a_{pi}\ln\Delta\overline{T}_i \tag{7}$$

$$\frac{\partial \Pi}{\partial w}=0: x\sum_{i=1}^{n}\ln v_i \ln(\bar{a}_{\mathrm{RMS}})_i + y\sum_{i=1}^{n}\ln v_{\mathrm{f}i} \ln(\bar{a}_{\mathrm{RMS}})_i + z\sum_{i=1}^{n}\ln a_{\mathrm{p}i}(\bar{a}_{\mathrm{RMS}})_i + w\sum_{i=1}^{n}\ln(\bar{a}_{\mathrm{RMS}})_i^2 + \eta\sum_{i=1}^{n}\ln(\bar{a}_{\mathrm{RMS}})_i = \sum_{i=1}^{n}\ln(\bar{a}_{\mathrm{RMS}})_i \ln\Delta\bar{T}_i \tag{8}$$

$$\frac{\partial \Pi}{\partial \eta}=0: x\sum_{i=1}^{n}\ln v_i + y\sum_{i=1}^{n}\ln v_{fi} + z\sum_{i=1}^{n}\ln a_{pi} + w\sum_{i=1}^{n}\ln(\bar{a}_{\mathrm{RMS}})_i + \eta\sum_{i=1}^{n}1 = \sum_{i=1}^{n}\ln\Delta\bar{T}_i \tag{9}$$

Eqs.(5)-(9) can be transformed into linear equations about x, y, z, w, η, and then we take the three cutting parameters, the measured value $\Delta\bar{T}$ and acceleration characteristic value $\bar{a}_{\mathrm{RMS}}$ of a certain direction vibration into formula (5) ~ (9), thus the undetermined parameters x, y, z, w, C (C=e$^{\eta}$) can be solved by MATLAB software programming.

Then take the obtained regression coefficients C, x, y, z, w into the formula (2), we can develop the fitting temperature rise $\Delta\tilde{T}_a$, $\Delta\tilde{T}_r$, $\Delta\tilde{T}_t$ corresponding to axial vibration, radial vibration and tangential vibration respectively, we have

$$\begin{aligned}\Delta\tilde{T}_a &= C_1 v^{x_1} v_{\mathrm{f}}^{y_1} a_{\mathrm{p}}^{z_1} \bar{a}_{\mathrm{RMS}\text{-}a}^{w_1}\\ \Delta\tilde{T}_r &= C_2 v^{x_2} v_{\mathrm{f}}^{y_2} a_{\mathrm{p}}^{z_2} \bar{a}_{\mathrm{RMS}\text{-}r}^{w_2}\\ \Delta\tilde{T}_t &= C_3 v^{x_3} v_{\mathrm{f}}^{y_3} a_{\mathrm{p}}^{z_3} \bar{a}_{\mathrm{RMS}\text{-}t}^{w_3}\end{aligned} \tag{10}$$

Where C_i, x_i, y_i, z_i, w_i, i=1,2,3, are the undetermined parameters corresponding to three-way vibration. Then the correlation coefficient is calculated by [R,P]=corrcoef (x,y) program of MATLAB, where R represents the correlation coefficient between $\Delta\tilde{T}$ and $\Delta\bar{T}$, and P represents the probability value of zero correlation. The calculation results of three kinds cutting tools are shown in Tables 7.

Table 7 Regression model parameters and correlation coefficients for three tools

Cutter tool	direction	C_i	x_i	y_i	z_i	w_i	R	P
D1	axial	1.37e-05	1.42	1.15	2.53	-0.16	0.78	1.05 e-08
	radial	1.16e-05	1.43	1.17	2.58	-0.26	0.8	3.82e-08
	tangential	1.23e-05	1.43	1.16	2.54	-0.1	0.79	1.32e-08
D2	axial	6.24e-05	0.80	1.81	1.61	0.45	0.73	4.28e-07
	radial	3.95e-05	0.84	1.83	1.58	0.79	0.75	8.65e-08
	tangential	7.60e-05	0.79	1.76	1.6	0.39	0.73	2.29e-06
D3	axial	0.197	0.60	1.15	0.67	1.12	0.74	5.62e-05
	radial	0.0952	0.58	0.76	0.61	1.08	0.73	9.61e-04
	tangential	0.2273	0.50	0.66	0.68	1.32	0.74	5.47e-04

According to Table 7, the correlation coefficient of D1 is higher than that of D3 and D2, and the probability P value of tool D1 correlation of 0 is less than that of tools D2 and D3, which means that the cutting vibration of tool D1 has a very good correlation with the cutting

temperature rise, which can be used to predict the measured cutting temperature of the tool very well. The fitting correlation of the radial vibration of the three tools is relatively high, indicating that the cutting temperature changes of the tools will have a certain influence on the radial vibration of cutting.

3.5.2 The fitting model of cutting vibration by cutting temperature rise and cutting parameters

In order to analyze the effect of cutting temperature rise and cutting parameters on cutting vibration, here we use the average cutting temperature rise $\Delta\overline{T}$ and three cutting parameters as variables to establish a fitting model for predicting the root-mean-square value of cutting vibration acceleration $\overline{a}_{\mathrm{RMS}}$, namely

$$\tilde{a}_{\mathrm{RMS}} = C' v^{x'} v_{\mathrm{f}}^{y'} a_{\mathrm{p}}^{z'} \Delta\overline{T}^{w'}$$

Then for the three directional vibration, let

$$\begin{aligned} \tilde{a}_{\mathrm{RMS}\text{-}a} &= C_1' v^{x_1'} v_{\mathrm{f}}^{y_1'} a_{\mathrm{p}}^{z_1'} \Delta\overline{T}^{w_1'} \\ \tilde{a}_{\mathrm{RMS}\text{-}r} &= C_2' v^{x_2'} v_{\mathrm{f}}^{y_2'} a_{\mathrm{p}}^{z_2'} \Delta\overline{T}^{w_2'} \\ \tilde{a}_{\mathrm{RMS}\text{-}t} &= C_3' v^{x_3'} v_{\mathrm{f}}^{y_3'} a_{\mathrm{p}}^{z_3'} \Delta\overline{T}^{w_3'} \end{aligned} \tag{11}$$

where $\tilde{a}_{\mathrm{RMS}\text{-}a}$, $\tilde{a}_{\mathrm{RMS}\text{-}r}$, $\tilde{a}_{\mathrm{RMS}\text{-}t}$ is the fitted value of the root-mean-square value of unidirectional acceleration corresponding to axial vibration, radial vibration and tangential vibration respectively.

By the same method as in Section 3.5.1, we can solve the undetermined coefficients $x_i', y_i', z_i', w_i', C_i'$ (i=1,2,3) in Eq.(11).

And the correlation coefficient between the predicted value $\tilde{a}_{\mathrm{RMS}}$ and the measured value $\overline{a}_{\mathrm{RMS}}$ can be calculated as shown in Table 8.

Table 8 Regression model parameters and correlation coefficients for three tools

Cutter tool	direction	C_i'	x_i'	y_i'	z_i'	w_i'	R	P
D1	axial	0.69	0.05	-0.02	0.06	-0.04	0.23	0.18
	radial	0.16	0.21	0.18	4.60	-0.11	0.40	0.02
	tangential	0.28	0.16	0.04	0.20	-0.03	0.23	0.17
D2	axial	12.40	-0.16	-0.40	-0.09	0.48	0.63	3.3e-05
	radial	11.15	-0.18	-0.34	-0.10	0.07	0.50	1.9e-03
	tangential	10.58	-0.16	-0.34	-0.08	0.04	0.54	5.1e-04
D3	axial	17.89	-0.25	-0.77	-0.40	0.39	0.71	1.4e-03
	radial	4.78	-0.25	-0.44	-0.37	0.42	0.62	7.0e-03
	tangential	1.86	-0.15	-0.29	-0.36	0.35	0.68	2.4e-04

According to Table 8, the correlation coefficients of tools D1 and D2 are relatively low,

indicating that the change of cutting temperature has no significant effect on cutting vibration; for tool D3, the correlation coefficients are all greater than 0.6, and the correlation with axial vibration fitting is relatively high, indicating that the cutting temperature changes of severely worn tools will have a certain effect on the cutting axial vibration.

4 Conclusions

The cutting experiments of the tools with the same cutting parameters and the same workpiece size were completed for three kinds of tools with different wear states. The cutting temperature and cutting vibration near the tool tip were collected synchronously, and the mutual coupling characteristics of tool cutting heat and cutting vibration under different wear states were studied. research shows:

(1) The cutting temperature of the severely worn tool has the highest correlation with the cutting parameters, and the new tool has the lowest correlation, indicating that the more severely worn tools are affected by the cutting temperature more significantly.

(2) Cutting parameters have the most significant impact on cutting vibration of severely worn tools, while moderately worn tools are the least affected.

(3) Based on the cutting vibration and cutting parameters, a fitting model of the average cutting temperature rise is established. This model can better predict the average cutting temperature rise of the tool under the given cutting parameters. Based on the cutting temperature changes and cutting parameters, a prediction model of cutting vibration is established, and the correlation calculation shows that the cutting heat of tools D1 and D2 has a weak effect on the cutting vibration.

(4) In the experimental data, there is a sharp rise and a sharp drop in the cutting temperature, and especially when the severely worn tool adopts larger cutting parameters, the cutting temperature is too high, smoke appears, and the test is forced to stop. The possible reason is that the chips did not fall off in time when the tool was cutting the workpiece, which resulted in the accumulation of chips, which caused a large change in the cutting temperature.

(5) The wear state of the three cutting tools is obtained through observation, and the division of the tool wear state is further studied in the follow-up.

References

[1] Yu Q, Li S C, Zhang X, Shao M H (2019) Experimental study on correlation between cutting temperature rise and turning vibration in dry turning on aluminum alloy. Int J Adv Manuf Technol 103:453-469.

[2] Zhang R R, Li C H, Zhao X F, et al (2016) The influence of tool geometric parameters on the turning performance of aluminum alloy. Machinery (In China) 43 (2): 1-4 + 52.

[3] Majumdar P, Jayaramachandran R. Ganesan S (2005) Finite element analysis of temperature rise in metal cutting processes Appl Therm Eng 25: 2152–2168.

[4] Karaguzel U, Bakkal M, Budak E (2016) Modeling and Measurement of Cutting Temperatures in Milling. Procedia CIRP 46:173-176.

[5] Cui X, Guo J (2017) Effects of cutting parameters on tool temperatures in intermittent turning with the formation of serrated chip considered. Appl Therm Eng 110:1220-1229.

[6] Chinchanikar S, Choudhury S K (2014) Evaluation of Chip-tool Interface Temperature: Effect of Tool Coating and Cutting Parameters during Turning Hardened AISI 4340 Steel. Procedia Mater. Sci. 6:996-1005.

[7] Liu P H, Jiang Z H, Wang X L (2013) Research on the simulation and experiment of cutting temperature in machining TC4 titanium alloy. Manufacturing Technology & Machine Tool (In China) 10:81-83+88.

[8] Li Y S, Deng J X, Zhang H, et al (2008) Study on wear mechanism of cemented carbide tool in high speed turning titanium alloy. Tribology Journal (In China) 28(5):443-447

[9] Zhang Y, Su H H, Fu Y C, et al (2014) Influence of tool material and wear on cutting temperature of turning titanium matrix composites. Aviation Precision manufacturing technology (In China) 10: 94-97.

[10] Shi W T, Hou Y J , Kong C, et al (2019) Optimization of cutting force and temperature during Ti6Al4V/Al7050 laminate composites elliptical vibration turning. J Mech Eng Sci 16:5585-5596

[11] Qu Z X, Zhang W L (2009) Model of temperature and turning force in NC turning of ultra-high strength steel. Tool Engineering (In China) 43(4):51-56.

[12] Shah D, Bhavsar S (2020) Effect of Tool Nose Radius and Machining Parameters on Cutting Force, Cutting Temperature and Surface Roughness an Experimental Study of Ti-6Al-4V (ELI) Mater Today: Proc 22 (2020):1977-1986.

[13] Turkes E, Erdem M, Gok K, Gok A (2020) Development of a new model for determine of cutting parameters in metal drilling processes. J Braz Soc Mech Sci Eng 42 (2):305-326.

[14] Luo H, Wang Y Q, Zhang P (2020) Effect of cutting and vibration parameters on the cutting performance of 7075-T651 aluminum alloy by ultrasonic vibration. Int J Adv Manuf Technol 107 (17):371-384.

[15] Maroju N, Vamsi K, Jin X (2017) Investigations on feasibility of low-frequency vibration-assisted turning. Int J Adv Manuf Technol 91(9-12):3775-3788.

[16] Li S C, Zhang Q, Wu M M (2016) Research on time-varying characteristics of torsion vibration mode for cutting workpiece. Modern Manufacturing Engineering (In China) 9:99-103.

[17] Chanda A, Dwivedy S K (2018) Nonlinear dynamic analysis of flexible workpiece and tool in turning operation with delay and internal resonance. J Sound Vib 434:358-378.

[18] Deshpande Y, Andhare A Sahu N (2017) Estimation of surface roughness using cutting parameters, force, sound, and vibration in turning of Inconel 718. J Braz Soc Mech Sci Eng 39 (12):5087-5096.

[19] Chen C, Chiang K, Chou C, et al (2011) The use of D-optimal design for modeling and analyzing the vibration and surface roughness in the precision turning with a diamond cutting tool. Int J Adv Manuf Technol 54(5-8):465-478.

[20] Hu J P, Yi T, Li K J, et al (2015) Modeling Simulation and Control of Turning Chatter Based on Variable Structure Parameters. Noise and Vibration Control (In China) 35(04):212-218.

[21] Cui Z, Chen N, Ji P, et al (2016) The influence of cutting amount on cutting force and cutting vibration. Machine tools and hydraulic (In China) 44(7):10-13.

[22] Chuan X (2014). Study on vibration signal and recognition of tool wear conditions. Public Communication of Science & Technology (In China) 16:65-68.

[23] Ozbek O, Saruhan H (2020) The effect of vibration and cutting zone temperature on surface roughness and tool wear in eco-friendly MQL turning of AISI D2. J Mater Res Technol 9(3):2762-2772.

[24] Prasad B S, Babu M P (2017) Correlation between vibration amplitude and tool wear in turning: Numerical and experimental analysis. Eng Sci Technol 20(1):197-211.

[25] Thomas M, Beauchamp Y (2003) Statistical investigation of modal parameters of cutting tools in dry turning. Int J Mach Tool Manu 43(11):1093-1106.

[26] Ghosh P, Chakraborty S, Biswas A R, et al (2018) Empirical Modelling and Optimization of Temperature and Machine Vibration in CNC Hard Turning. Mater Today: Proc 5(5):12394-12402.

[27] Upadhyay V, Jain P K, Mehta N K (2012) In-process prediction of surface roughness in turning of Ti–6Al–4V alloy using cutting parameters and vibration signals. Measurement 46(1):154-160.

[28] Liu Q M, Xu J K, Yu H (2020) Experimental study of tool wear and its effects on cutting process of ultrasonic-assisted milling of Ti6Al4V. Int J Adv Manuf Technol 108 (3):2917-2928.

[29] Mou W P, Zhu S W (2020) Vibration, tool wear and surface roughness characteristics in turning of Inconel 718 alloy with ceramic insert under LN2 machining. J Braz Soc Mech Sci Eng 42(1-2):1683-1691.

[30] Das D; Kumar S Pradhan; Sahoo A K, et al (2020), Satpathy M P, Samal C. Tool wear and cutting force investigations during turning 15 wt% SiCp -Al 7075 metal matrix composite. Mater Today: Proc 26(2):854-859.

[31] Fang Z L, Obikawa T (2018) Influence of cutting fluid flow on tool wear in high-pressure coolant turning using a novel internally cooled insert. J Manuf Process 56:1114-1125.

[32] Upase R, Ambhore N (2020). Experimental investigation of tool wear using vibration signals: An ANN approach. Mater Today: Proc 24(2):1365-1375.

[33] Dou J M, Xu C W, Jiao S J, et al (2020). An unsupervised online monitoring method for tool wear using a sparse auto-encoder. Int J Adv Manuf Technol 106(5):2493-2507

[34] Hong T T, Cuong N V, Ky L H, et al (2020). Multi-Criteria Optimization of Dressing Parameters for Surface Grinding 90CrSi Tool Steel Using Taguchi Method and Grey Relational Analysis. Mater Sci Forum 5970:61-68.

The author's statement

Ethical Approval: My research does not involve ethical issues.

Consent to Participate: My research does not involve ethical issues, it only involves aluminum alloy and other materials processing problems, and requires workers to process work-pieces.

Consent to Publish: All the authors agreed to publish this paper.

Authors Contributions: Songyuan Li：Write original manuscript and translate;

Shuncai Li：Revise the paper and verify the results;

Yuting Hu：Experiment, data collection, verifying;

Eugene Popov：Test and data processing.

All authors of this paper have read and approved the final version submitted.

Funding: This work was supported by the Postgraduate Research & Practice Innovation Program of Jiangsu Province (KYCX20_2331), Joint scientific research project of Sino foreign cooperative education platform in Jiangsu Province, the Science and Technology Plan Project of Xuzhou City (KC20188) and Undergraduate Innovation Training Program (201910320117Y).

Competing Interests: The authors declare that they have no competing interests.

Availability of data and materials: The data in this paper are all obtained from experiments. All data generated during this study are included in this manuscript.

Figures

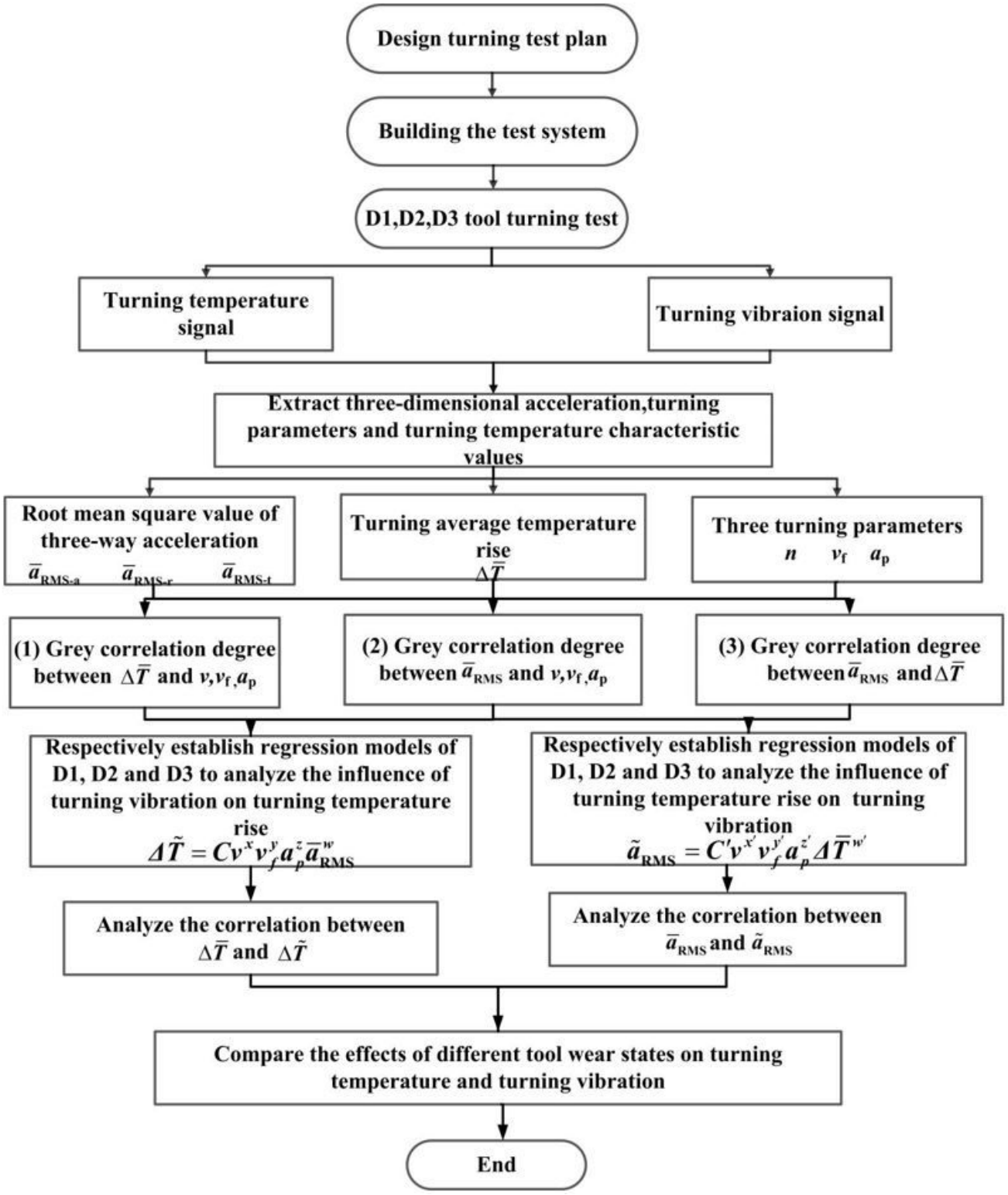

Figure 1

Research technology roadmap

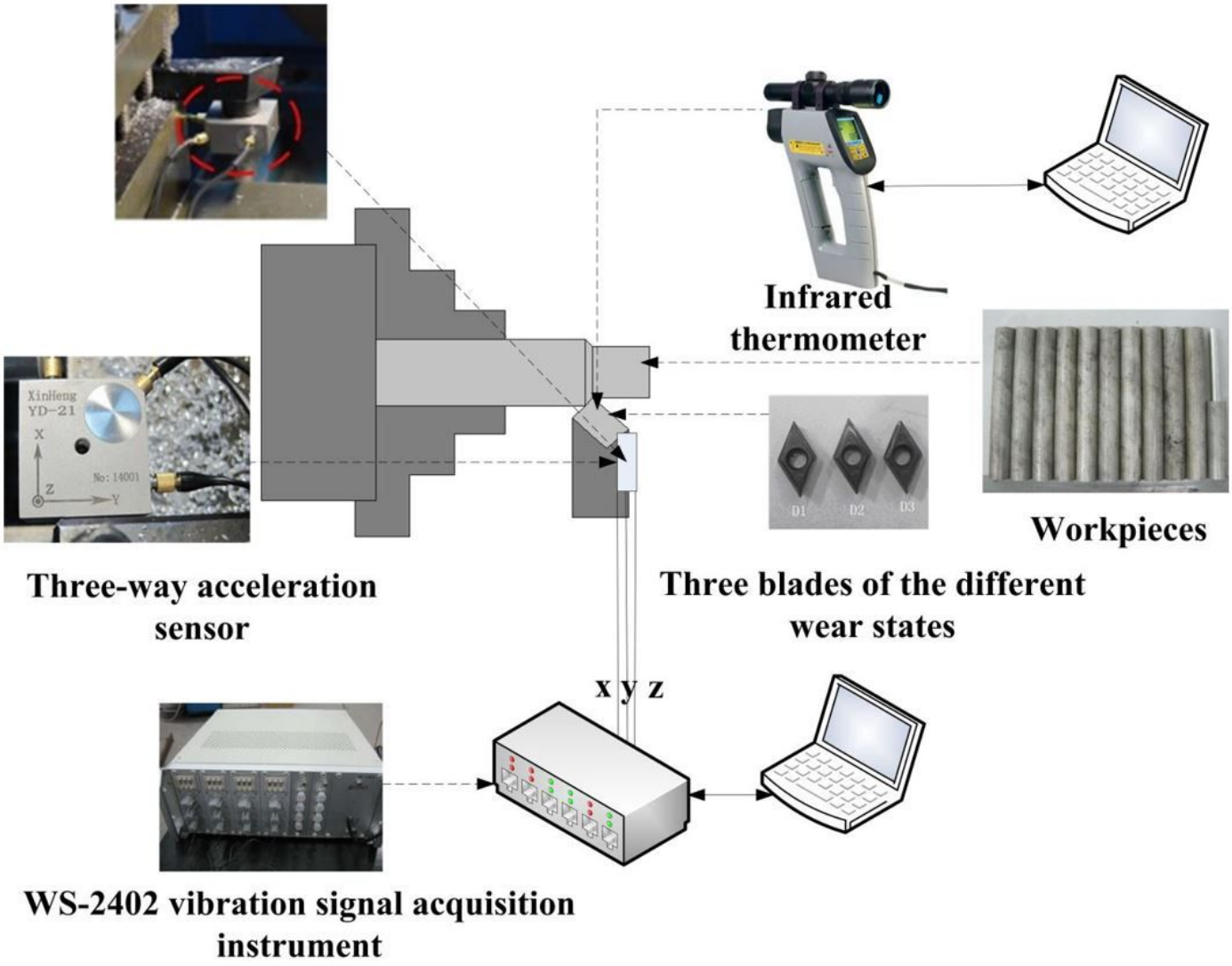

Figure 2

Cutting test system

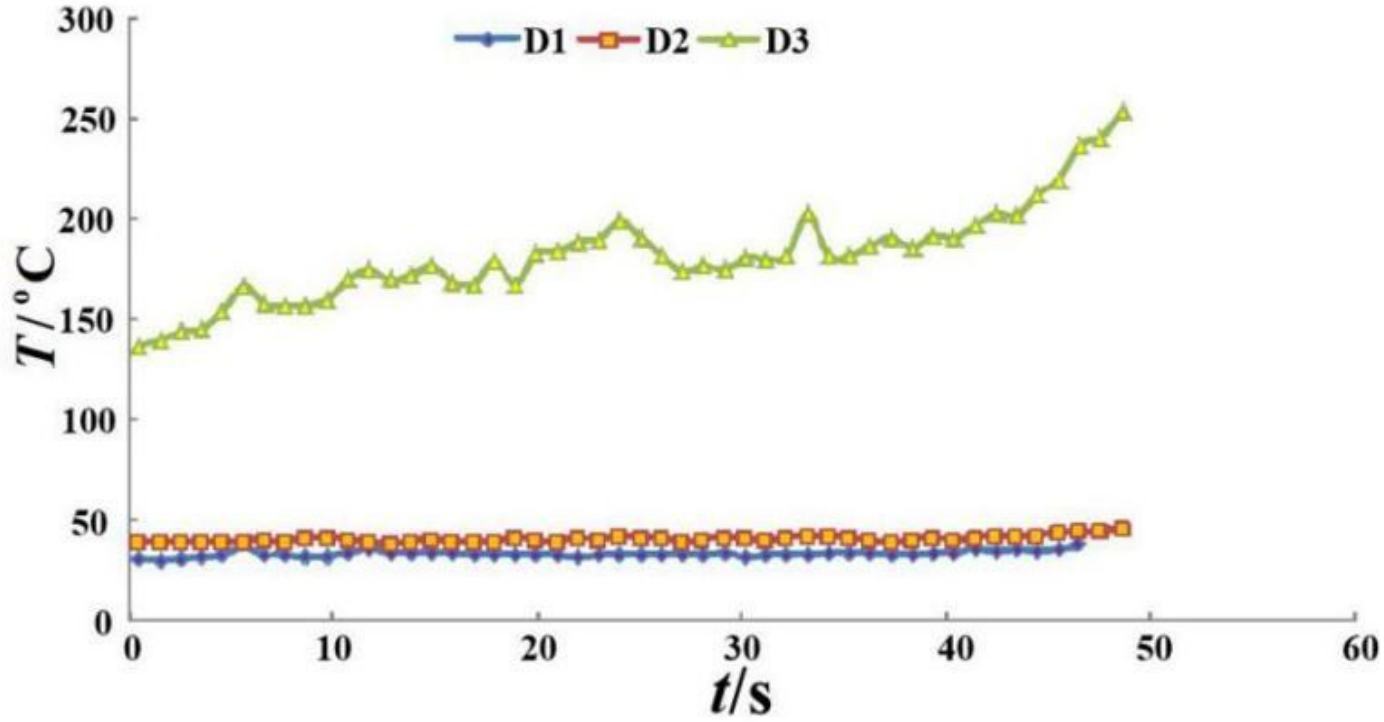

Figure 3

Time curves of cutting temperature of three tools at n=1200r/min, vf=80 mm/min, ap=0.3mm

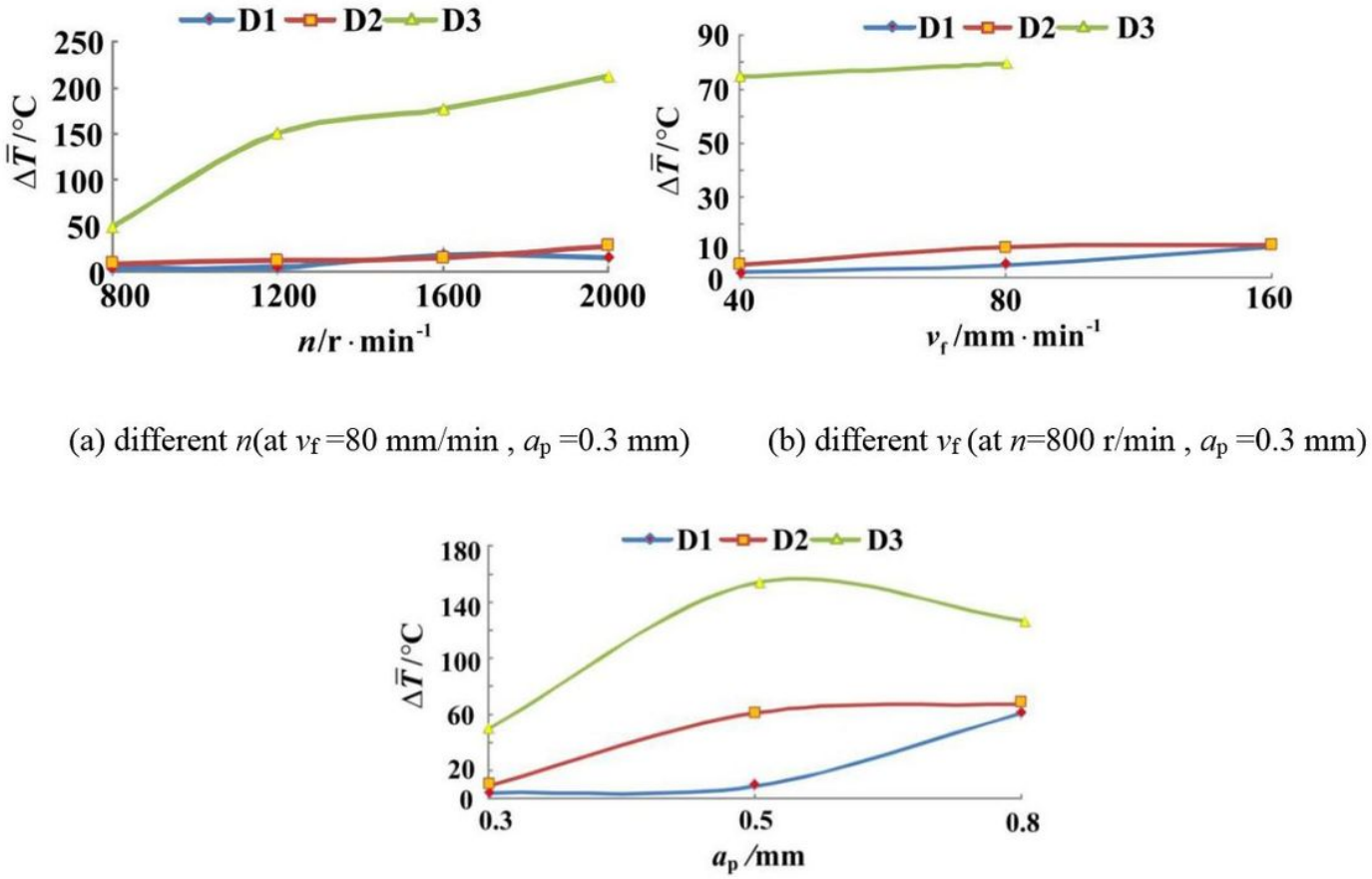

(a) different n(at v_f =80 mm/min , a_p =0.3 mm)

(b) different v_f (at n=800 r/min , a_p =0.3 mm)

(c) different a_p(at n=800 r/min ,v_f=80 mm/min)

Figure 4

Comparison curve of cutting temperature rise of 3 kinds of tools under different cutting parameters

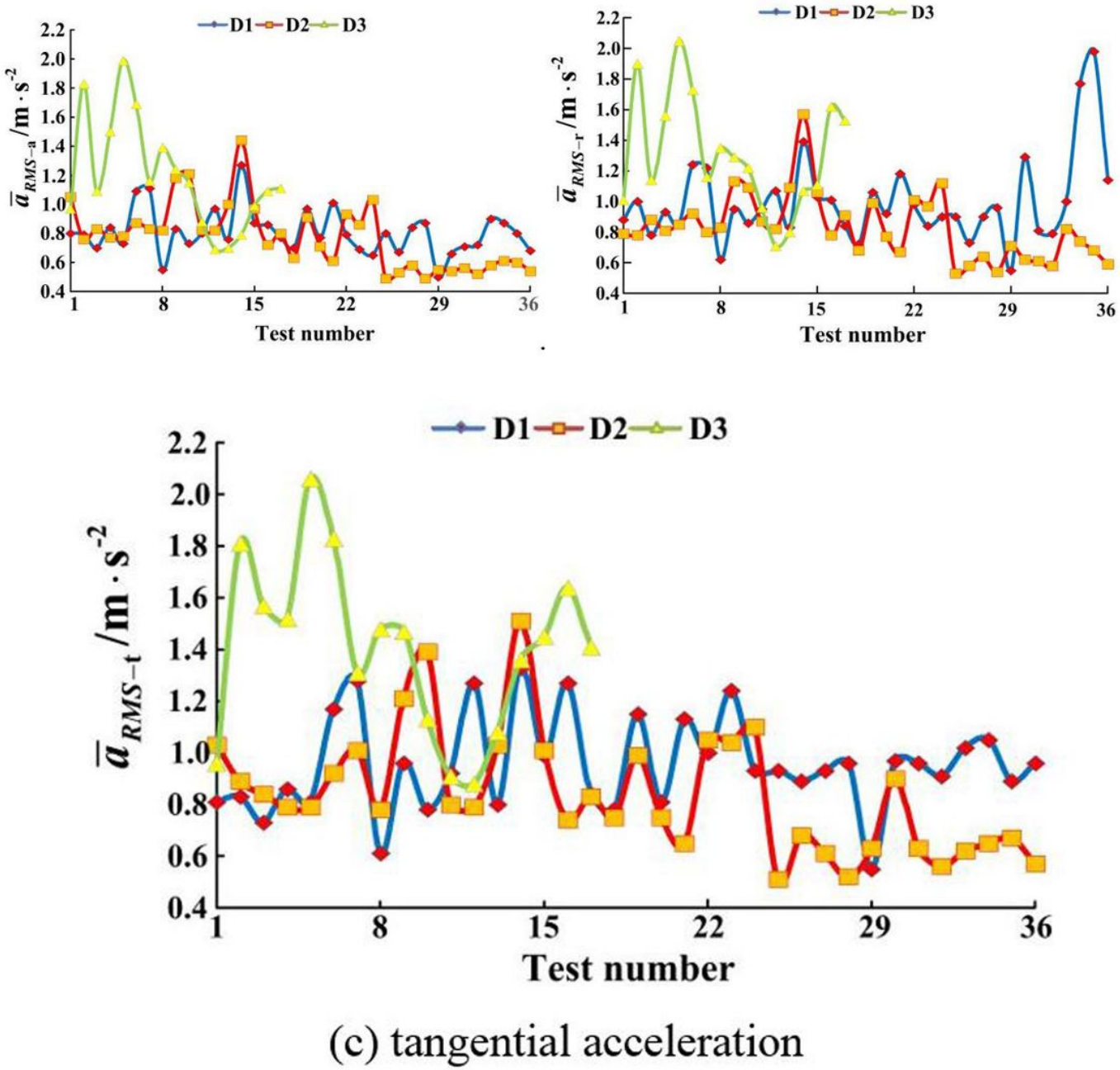

Figure 5

Comparing curves of acceleration mean square of all tests for three tools